



Title	Dislocation structure produced by an ultrashort shock pulse
Author(s)	Matsuda, Tomoki; Sano, Tomokazu; Arakawa, Kazuto et al.
Citation	Journal of Applied Physics. 2014, 116(18), p. 183506
Version Type	VoR
URL	https://hdl.handle.net/11094/89439
rights	This article may be downloaded for personal use only. Any other use requires prior permission of the author and AIP Publishing. This article appeared in Matsuda T., Sano T., Arakawa K., et al. Dislocation structure produced by an ultrashort shock pulse. Journal of Applied Physics, 116(18), 183506 and may be found at https://doi.org/10.1063/1.4901928 .
Note	

The University of Osaka Institutional Knowledge Archive : OUKA

<https://ir.library.osaka-u.ac.jp/>

The University of Osaka

Dislocation structure produced by an ultrashort shock pulse

Cite as: J. Appl. Phys. **116**, 183506 (2014); <https://doi.org/10.1063/1.4901928>

Submitted: 21 June 2014 • Accepted: 05 November 2014 • Published Online: 13 November 2014

Tomoki Matsuda (松田朋己), Tomokazu Sano (佐野智一), Kazuto Arakawa (荒河一渡), et al.



View Online



Export Citation



CrossMark

ARTICLES YOU MAY BE INTERESTED IN

[Multiple-shocks induced nanocrystallization in iron](#)

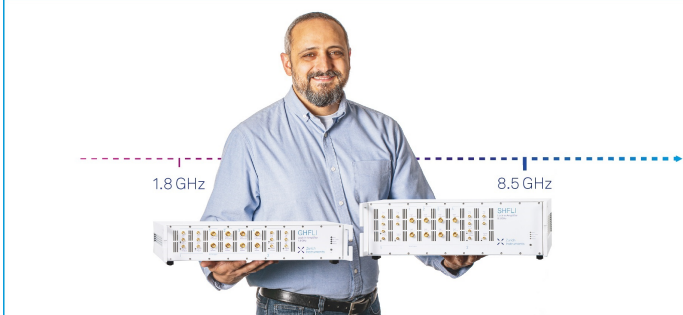
Applied Physics Letters **105**, 021902 (2014); <https://doi.org/10.1063/1.4890389>


[Femtosecond laser peening of 2024 aluminum alloy without a sacrificial overlay under atmospheric conditions](#)

Journal of Laser Applications **29**, 012005 (2017); <https://doi.org/10.2351/1.4967013>


[Synthesis of submicron metastable phase of silicon using femtosecond laser-driven shock wave](#)

Journal of Applied Physics **110**, 126103 (2011); <https://doi.org/10.1063/1.3673591>



Trailblazers. 

Meet the Lock-in Amplifiers that measure microwaves.

 Zurich Instruments [Find out more](#)

Dislocation structure produced by an ultrashort shock pulse

Tomoki Matsuda (松田朋己),^{1,a)} Tomokazu Sano (佐野智一),^{1,2}
 Kazuto Arakawa (荒河一渡),^{2,3} and Akio Hirose (廣瀬明夫)¹

¹*Division of Materials and Manufacturing Science, Graduate School of Engineering, Osaka University, Suita, Osaka 565-0871, Japan*

²*JST, CREST, Suita, Osaka 565-0871, Japan*

³*Department of Material Science, Interdisciplinary Faculty of Science and Engineering, Shimane University, Matsue, Shimane 690-8504, Japan*

(Received 21 June 2014; accepted 5 November 2014; published online 13 November 2014)

We found an ultrashort shock pulse driven by a femtosecond laser pulse on iron generates a different dislocation structure than the shock process which is on the nanosecond timescale. The ultrashort shock pulse produces a highly dense dislocation structure that varies by depth. According to transmission electron microscopy, dislocations away from the surface produce microbands via a network structure similar to a long shock process, but unlike a long shock process dislocations near the surface have limited intersections. Considering the dislocation motion during the shock process, the structure near the surface is attributed to the ultrashort shock duration. This approach using an ultrashort shock pulse will lead to understanding the whole process of shock deformation by clarifying the early stage. © 2014 AIP Publishing LLC.

[<http://dx.doi.org/10.1063/1.4901928>]

I. INTRODUCTION

The behavior of dislocations has attracted increased attention, because dislocations formed during the shock process are a dominant factor for plastic deformation of materials.^{1,2} The increase in dislocations that accompany the high-strain-rate deformation associated with the shock process is due to the generation of new dislocations rather than multiplication of existing dislocations.^{3–6} Both simulations using molecular dynamics^{7–9} or dislocation dynamics with a finite element framework^{10,11} and metallurgical analyses after the shock process using flyer plate impact^{12,13} or nanosecond laser pulse¹⁴ have been performed to clarify the dislocation behavior under shock deformation. However, the results are inconsistent; simulations deal with the early stage of the shock process (within one hundred picoseconds),^{7–9} whereas most metallurgical analyses deal with materials that undergo a shock process consisting of a compression and subsequent release.^{1,2} Consequently, metallurgical analysis after a shock process, which is on the nanosecond timescale, shows not the dislocation structure formed during the early compression, but the thermally recovered microstructure formed during the release process.^{15,16}

An ultrashort shock pulse can be produced using a femtosecond laser pulse. Plasma formation is initiated within several tens of picoseconds after the irradiation of a laser pulse above the fluence threshold,^{17–20} and a shock wave is produced due to the recoil force of plasma expansion. Some interferometric measurements (e.g., frequency-domain interferometry) have experimentally shown that 10%–90% rise time of the shock wave is 6.25 ps in several types of thin metal target,²¹ and the plastic wave with a compression

stress is 27.5 GPa behind the front of elastic precursor in a 250-nm-thick iron sample where fluence of the laser pulse is 3 J cm^{-2} .²² Additionally, simulations have investigated the evolution of the shock profile when the compression, which consists of an elastic shock wave and a plastic shock wave with approximately 90 GPa of pressure lasting several tens of picoseconds, attenuates with the propagation distance in nickel at a fluence of 1.57 J cm^{-2} .²³

The produced ultrashort shock pulse may suppress thermal recovery^{24–26} because the short duration and small thickness, where the shock exists, facilitate rapid cooling^{21–23,27} and consequently induce the absence of persistent heating. Compared to using a nanosecond laser pulse as a shock driver, the heat-affected region in femtosecond laser irradiated metals, which depends on the fluence, is much smaller (between 100 nm and $1 \mu\text{m}$).^{28,29} Additionally, the duration of shock pulse is extended following attenuation during shock propagation.^{1,2,22,23} Therefore, employing an ultrashort shock pulse should retain evidence of the dislocation structure formed during the early shock process near the surface and represent the transition of the dislocation structure, which evolves during extended shock duration corresponding to propagated distance. Consequently, an ultrashort shock pulse may provide a fundamental understanding of the deformation process during the shock process on an ultrashort timescale. The purpose of the present work is to investigate the dislocation structure formed after an ultrashort shock pulse driven by a femtosecond laser pulse based on microstructural observations of iron.

II. EXPERIMENT

Polycrystalline pure iron with purity of 99.99% was used as the specimen. The average grain size was $140 \mu\text{m}$ after annealing at 1123 K to recover the initial strain and to

^{a)}Author to whom correspondence should be addressed. Electronic mail: t-matsu@mapse.eng.osaka-u.ac.jp

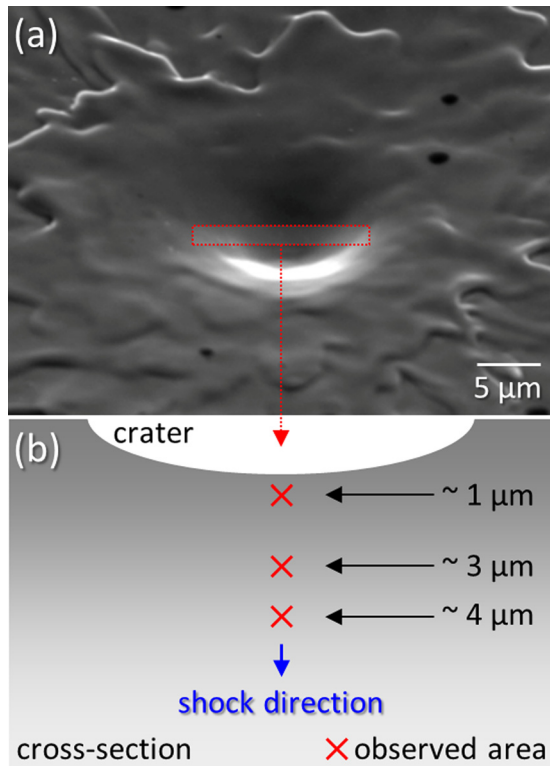


FIG. 1. Experimental (a) SEM image of iron irradiated with a femtosecond laser pulse. TEM specimen observed from the bottom of the crater. (b) Schematic illustration of the cross-section of TEM specimen. TEM observations were continuously performed along the shock direction.

coarsen the grain. A femtosecond laser (TSA; Spectra-Physics, Inc.) pulse with a wavelength of 800 nm, a pulse duration of 130 fs at full width at half maximum, and a pulse energy of 10 mJ was focused on a mirror-finished surface with a spot diameter of 100 μm . The average fluence of the laser pulse was about 130 J cm^{-2} , which drives an ultrashort shock pulse with a pressure above several tens of GPa. Figure 1(a) shows a scanning electron microscopy (SEM) image of the surface after laser irradiation with a femtosecond laser pulse; a deep crater with a depth of 4.95 μm is formed in a 20 μm area within the 100 μm spot size.

Since the shock wave is driven due to the recoil force of plasma expansion during the ablation, a higher stress is applied to the center of the crater, promoting a higher-strain-

rate deformation. A specimen was picked up from the bottom of the crater and thinned up to 100 nm for cross-sectional TEM (JEM-2010; JEOL) observations by using a focused ion beam instrument. Cross-sectional bright field TEM observations were performed continuously from surface to deeper region along the shock direction. The incident beam direction is nearly parallel to [110] at $\mathbf{g} = \bar{1}10$ (\mathbf{g} : reciprocal lattice vector), where the ratio of dislocations imaged in the observation is constant. TEM images at 1 μm (Regions A, B), 3 μm (Region C), 4 μm (Region D) from the surface are extracted (Fig. 1(b)).

III. RESULTS

Figures 2(a)–2(c) show TEM images within 1.5 μm from the surface after applying a shock pulse, enlarged view of Region A, and enlarged view of Region B, respectively. The dislocation structure varies by region, although areas below 500 nm from the outermost surface layer contain a similar density of dislocations. In Region A, individual dislocations are distinct with little overlap, whereas dislocations in Region B are entangled locally. These results indicate that the dislocation structure in Region A is not as evolved as those in Region B. (Hereafter, the not-as-evolved dislocation structure is referred to as the non-evolved dislocation structure.) This non-evolved dislocation structure differs from the one after a shock pulse on the nanosecond timescale.^{6–9} In addition, the difference in the dislocation structure at approximately several 100 nm from the surface indicates a change in the shock parameter, which influences the accumulation of dislocations.

Figure 3(a) shows TEM images observed in the deeper region corresponding to 3 μm (Region C) and Fig. 3(b) shows enlarged view of Region C. Region C shows existence of a density of dislocations as well as region B, but Region C contains more intersecting points between the dislocations than Region B, which form a uniform network structure.

Figure 4(a) shows a TEM image observed 4 μm from the surface (Region D). Region D contains unidirectional dislocation pile-ups, where the microstructure is divided into two regions: high- and low-density regions. Figure 4(b) shows a zoomed-out image, where the periodic dislocation pile-ups form a microband structure. These results indicate

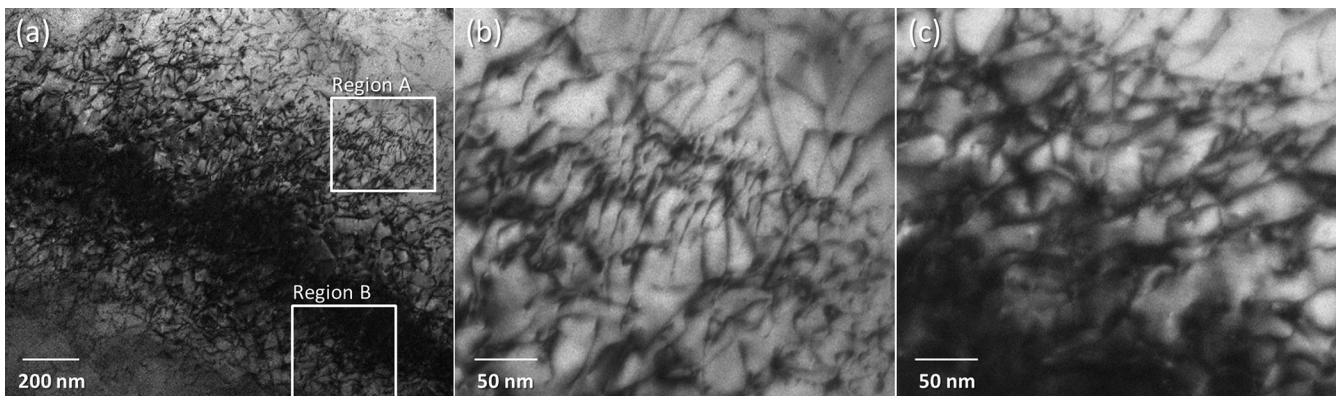


FIG. 2. TEM images near the surface after an ultrashort shock pulse. (a) General image within 1.5 μm from the surface. (b) Enlarged view corresponding to region A, which shows few overlapping dislocations. (c) Enlarged view corresponding to region B, which shows a local dislocation tangle.

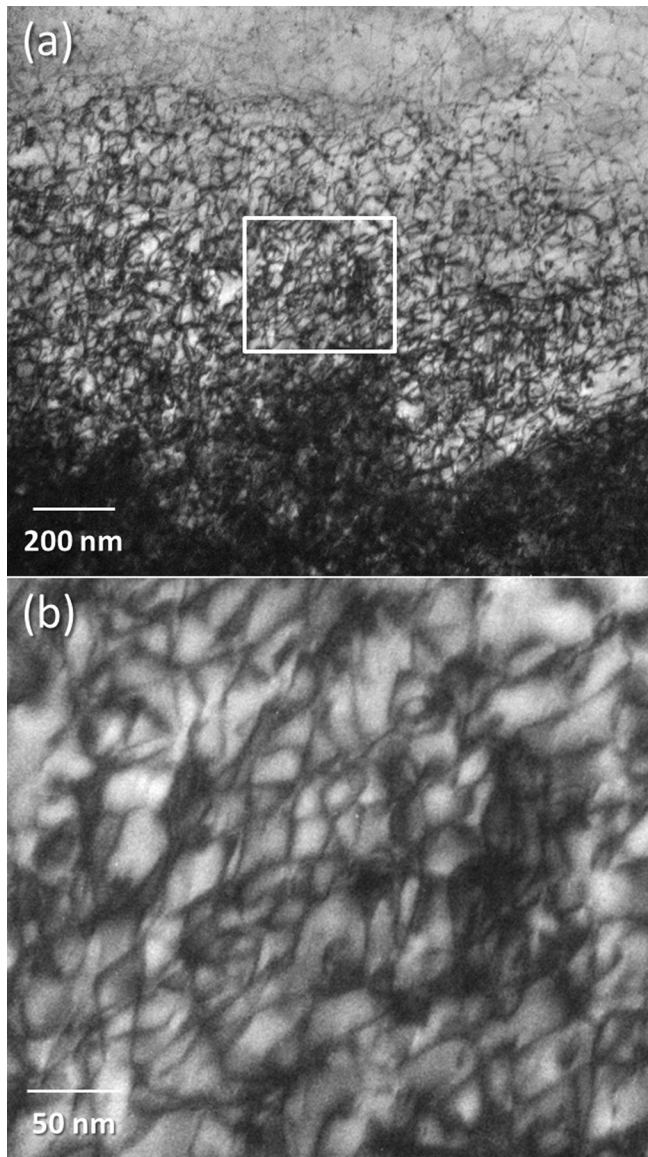


FIG. 3. TEM image observed 3 μm from the surface after an ultrashort shock pulse. (a) General image. (b) Enlarged view showing a uniform dislocation network structure.

that there is a transition in the dislocation structure from a network to a microband structure, revealing a crucial evolution in the dislocation structures due to mutual interactions with depth against little evolution within 1.5 μm .

The evolved dislocation structures, such as microband, are generally formed in plastically deformed body-centered-cubic structure.³⁰ In addition, a shock process lasting longer than a nanosecond or a high-strain-rate deformation induces evolved structures in highly stressed regions, but as the depth increases, these structures disappear and the dislocations do not interact. Consequently, the transition of the dislocation structure from Region A to Region D induced by an ultrashort shock pulse differs significantly from that induced by a longer shock pulse.

IV. DISCUSSION

Both strain and temperature determine the evolution of dislocation structures during plastic deformation of metals.

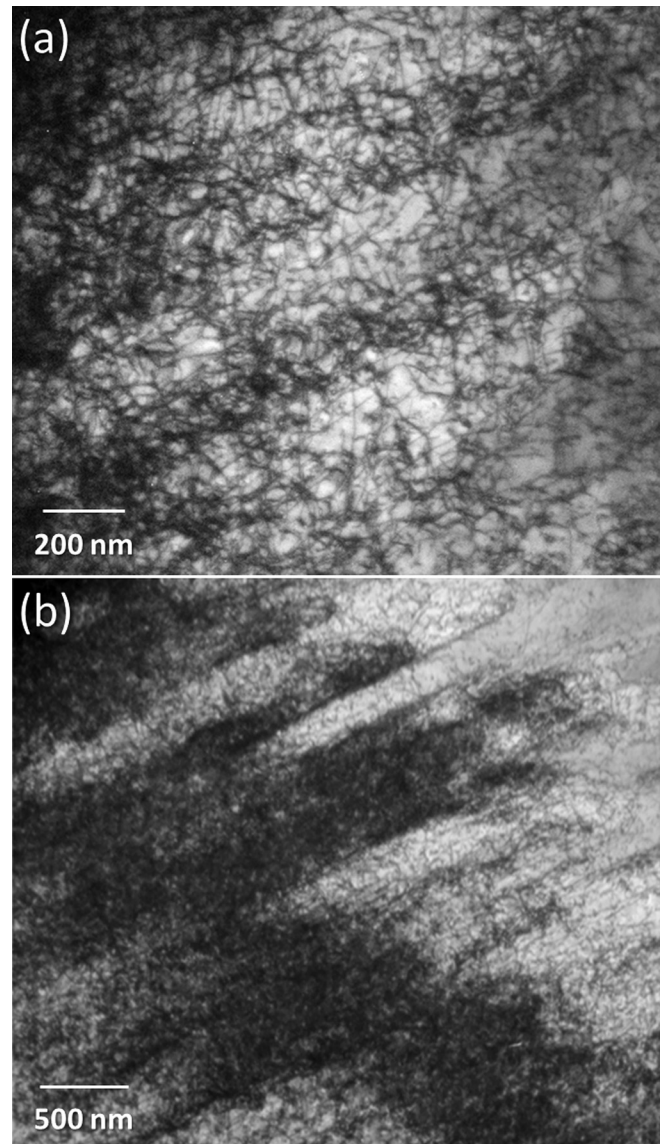


FIG. 4. TEM images of iron 4 μm below the surface after an ultrashort shock pulse. (a) Image showing a dislocation pile-up. (b) Zoom-out image showing the periodic microband structure consisting of the dislocation pile-ups.

Because the evolution of the dislocation structure can be promoted due to thermal recovery during temperature drop after shock loading, the influence of the temperature associated with the shock process on the dislocation structure should be considered.¹⁰ We evaluated the dislocation density at each region to determine the effects of a shock pulse on the picosecond scale using the Ham equation,³¹ which is expressed as $\rho = 2N/Lt$, where ρ is the dislocation density, N is the number of intersecting points between the dislocation lines and grid lines drawn on the TEM micrograph, L is the total length of the grid lines, and t is the thickness of the TEM sample. Consequently, Regions A to D (at a microband) exhibit dislocation densities of $(2.8 \pm 0.4) \times 10^{15}$, $(1.8 \pm 0.2) \times 10^{15}$, $(2.7 \pm 0.1) \times 10^{15}$, and $(1.8 \pm 0.2) \times 10^{15} \text{ m}^{-2}$, respectively. Regions A and C have maximum dislocation densities of around $3 \times 10^{15} \text{ m}^{-2}$, but there is not an obvious difference corresponding to the change of dislocation structure. Despite the higher stress involving more increase in temperature, which should promote evolution, the

dislocation structure is not evolved near the surface, indicating that influence of temperature increase on the evolution of the dislocation structure can be neglected in ultrashort shock process. Additionally, the results suggest that the density of the dislocations is due to different mechanisms in different regions.

We discuss the relation between the strain and the dislocation structure. Deformed metals show several stages of microstructural evolution as the strain increases:³⁰ the dislocation motion on the slip plane, evolution of the tangle and cell structure, and formation of a dislocation wall and subsequent structure due to dynamic recovery. Thus, dislocation structures evolve due to the mutual interactions and intersections due to sufficient dislocation motion during a shock after an increase in strain. Decrease in shock duration inhibits evolution of dislocation structure, such as dislocation cells, due to less interaction between dislocations for a short time.⁶ Dislocation structures evolved in longer shock processes appear to correspond to the structure subsequent to that in the second stage.

It is generally assumed that dislocations cannot exceed the speed of sound in a shear wave due to the infinite dislocation self-energy.³² Here, we show a simple calculation to determine the distance that individual dislocations move as the shock pulse passes by assuming that the dislocation velocity is equal to the speed of sound (3260 m/s in iron³³). Additionally, the duration of shock pulse is assumed to be 50 ps at the early stage of shock wave generation from shock duration data.²⁵ Therefore, the calculated motion of a dislocation is about 160 nm, which is much shorter than the distance between the periodic dislocation pile-ups. This is why a small dislocation motion inhibits the interactions with other obstacles in the ultrashort duration of stress. As the shock wave propagates, the duration of the shock pulse increases, eventually reaching the nanosecond scale. Assuming that the dislocation velocity is on the same order, the distance exceeds 1 μm , which reveals that the dislocation interactions are sufficiently satisfied.

Increase in dislocation density during shock process is attributed to both multiplication and generation due to lattice mismatch before and behind the shock front.^{2,4,6} It has been also reported that homogenous nucleation of dislocations becomes predominant as the density increases for a short rise time compared to that for a long rise time.¹¹ Dislocation multiplication due to dislocation interactions may be the main factor for a high density of dislocations in the deeper region, but is not a factor near the surface. Therefore, we suggest that the high density of dislocations in non-evolved dislocation structures is due to dislocation nucleation, and that the observed structures are produced at an early stage of the shock process.

V. CONCLUSIONS

In summary, TEM observations identified a little intersected dislocation structure produced near the surface by an ultrashort shock pulse using a femtosecond laser pulse. Although there is not an obvious change in the dislocation density, the dislocation structure changes with depth from dislocations with little interactions near the surface to

microbands via a network structure further from the surface. The dislocation structure in the deeper region corresponds to that achieved during longer (on the nanosecond scale) shock processes, but the little intersected structure does not. Considering the dislocation motion during an ultrashort shock pulse, the motion of dislocations is around 160 nm, which is much shorter than the distance between microbands. Thus, we suggest that the little intersected dislocation structure is due to the ultrashort shock duration, which is typically produced during the early stage of the shock process. This approach using an ultrashort shock pulse should help elucidate the shock deformation process by clarifying the early stage of the shock process.

ACKNOWLEDGMENTS

The authors wish to thank Professor Narumi Inoue and Professor Masayuki Okoshi of National Defense Academy of Japan for their support of the laser irradiation experiments. This work was supported in part by JSPS KAKENHI Grant Nos. 22224012 and 25420778.

¹*Shock Waves and High-Strain-Rate Phenomena in Metals*, edited by M. A. Meyers and L. E. Murr (Plenum, New-York, 1981).

²M. A. Meyers, H. Jarmakani, E. M. Bringa, and B. A. Remington, in *Dislocations in Solids*, edited by J. P. Hirth and L. Kubin (North-Holland, Amsterdam, 2009), Vol. 15, Chap. 89, p. 91.

³E. Orowan, *Proc. Phys. Soc. London* **52**, 8 (1940).

⁴C. S. Smith, *Trans. Metal. Soc. AIME* **212**, 574 (1958).

⁵E. Hornbogen, *Acta Metall.* **10**, 978 (1962).

⁶M. A. Meyers, *Scr. Metall.* **12**, 21 (1978).

⁷T. C. Germann, B. L. Holian, P. S. Lomdahl, D. Tanguy, M. Mareschal, and R. Ravelo, *Mater. Trans. A* **35**, 2609 (2004).

⁸E. M. Bringa, K. Rosolankova, R. E. Rudd, B. A. Remington, J. S. Wark, M. Duchaineau, D. H. Kalantar, J. Hawrelak, and J. Belak, *Nature Mater.* **5**, 805 (2006).

⁹A. Higginbotham, M. J. Suggit, E. M. Bringa, P. Erhart, J. A. Hawrelak, G. Moggi, N. Park, B. A. Remington, and J. S. Wark, *Phys. Rev. B* **88**, 104105 (2013).

¹⁰M. A. Shehadeh, H. M. Zbib, and T. Diaz de la Rubia, *Philos. Mag.* **85**, 1667 (2005).

¹¹M. A. Shehadeh, E. M. Bringa, H. M. Zbib, J. M. McNaney, and B. A. Remington, *Appl. Phys. Lett.* **89**, 171918 (2006).

¹²L. E. Murr and D. Kuhlmann-Wilsdorf, *Acta Metall.* **26**, 847 (1978).

¹³G. T. Gray III, P. S. Follansbee, and C. E. Frantz, *Mater. Sci. Eng., A* **111**, 9 (1989).

¹⁴C. H. Lu, B. A. Remington, B. R. Maddox, B. Kad, H. S. Park, S. T. Prisbrey, and M. A. Meyers, *Acta Mater.* **60**, 6601 (2012).

¹⁵S. Mahajan, *Phys. Status Solidi* **33**, 291 (1969).

¹⁶H. N. Jarmakani, E. M. Bringa, P. Erhart, B. A. Remington, Y. M. Wang, N. Q. Vo, and M. A. Meyers, *Acta Mater.* **56**, 5584 (2008).

¹⁷J. P. Colombier, P. Combis, F. Bonneau, R. Le Harzic, and E. Audouard, *Phys. Rev. B* **71**, 165406 (2005).

¹⁸P. Zhu, Z. Zhang, L. Chen, J. Zheng, R. Li, W. Wang, J. Li, X. Wang, J. Cao, D. Qian, Z. Sheng, and J. Zhang, *Appl. Phys. Lett.* **97**, 211501 (2010).

¹⁹Z. Wu, X. Zhu, and N. Zhang, *J. Appl. Phys.* **109**, 053113 (2011).

²⁰C. Wu and L. V. Zhigilei, *Appl. Phys. A* **114**, 11 (2014).

²¹K. T. Gahagan, D. S. Moore, D. J. Funk, R. L. Rabie, and S. J. Buelow, *Phys. Rev. Lett.* **85**, 3205 (2000).

²²B. J. Demaske, V. V. Zhakhovsky, N. A. Inogamov, and I. I. Oleynik, *Phys. Rev. B* **87**, 054109 (2013).

²³S. I. Ashtikov, P. S. Komarov, M. B. Agranat, G. I. Kanel, and V. E. Fortov, *JETP Lett.* **98**, 384 (2013).

²⁴T. Sano, H. Mori, E. Ohmura, and I. Miyamoto, *Appl. Phys. Lett.* **83**, 3498 (2003).

²⁵T. Matsuda, T. Sano, K. Arakawa, and A. Hirose, *Appl. Phys. Lett.* **105**, 021902 (2014).

²⁶A. Vailionis, E. G. Gamaly, V. Mizeikis, W. Yang, A. V. Rode, and S. Juodkazis, *Nat. Commun.* **2**, 445 (2011).

- ²⁷S. D. McGrane, D. S. Moore, D. J. Funk, and R. L. Rabie, *Appl. Phys. Lett.* **80**, 3919 (2002).
- ²⁸R. L. Harzic, N. Huot, E. Audouard, C. Jonin, P. Laporte, S. Valette, A. Frackiewicz, and R. Fortunier, *Appl. Phys. Lett.* **80**, 3886 (2002).
- ²⁹J. P. Colombier, P. Combis, R. Stoian, and E. Audouard, *Phys. Rev. B* **75**, 104105 (2007).
- ³⁰A. S. Argon, *Strengthening Mechanisms in Crystal Plasticity* (Oxford University Press, Oxford, 2008), p. 283.
- ³¹R. K. Ham, *Philos. Mag.* **6**, 1183 (1961).
- ³²J. Friedel, *Dislocations* (Addison-Wesley, New-York, 1964), p. 63.
- ³³*Los Alamos Shock Wave Profile Data*, edited by C. E. Morris (University of California Press, Berkeley, 1982), p. 26.